

The EIF4EBP1 gene encoding 4EBP1 is transcriptionally upregulated by MYC and linked to shorter survival in medulloblastoma

Laura Hruby, Katerina Schaal, Alberto Delaidelli, Daniel Picard, Christopher Dunham, Oksana Lewandowska, Tobias Reiff, Magalie Larcher, Celio Pouponnot, Poul HB Sorensen, Barak Rotblat, Guido Reifenberger, Marc Remke & Gabriel Leprivier

Article - Version of Record

Suggested Citation:

Hruby, L., Schaal, K., Delaidelli, A., Picard, D., Dunham, C., Lewandowska, O., Reiff, T., Larcher, M., Pouponnot, C., Sorensen, P. H., Rotblat, B., Reifenberger, G., Remke, M., & Leprivier, G. (2025). The EIF4EBP1 gene encoding 4EBP1 is transcriptionally upregulated by MYC and linked to shorter survival in medulloblastoma. Cell Death Discovery, 11, Article 330. https://doi.org/10.1038/s41420-025-02601-x

Wissen, wo das Wissen ist.



This version is available at:

URN: https://nbn-resolving.org/urn:nbn:de:hbz:061-20251031-104829-2

Terms of Use:

This work is licensed under the Creative Commons Attribution 4.0 International License.

For more information see: https://creativecommons.org/licenses/by/4.0



ARTICLE OPEN



The *EIF4EBP1* gene encoding 4EBP1 is transcriptionally upregulated by MYC and linked to shorter survival in medulloblastoma

Laura Hruby^{1,12}, Katerina Schaal^{2,12}, Alberto Delaidelli^{3,4,5}, Daniel Picard^{1,2,6,7}, Christopher Dunham⁴, Oksana Lewandowska^{1,8}, Tobias Reiff ⁸, Magalie Larcher⁹, Celio Pouponnot⁹, Poul HB Sorensen^{3,4}, Barak Rotblat ^{10,11}, Guido Reifenberger^{1,6}, Marc Remke^{1,2,6,7} and Gabriel Leprivier ¹⁸

© The Author(s) 2025

Medulloblastoma (MB) is the most common malignant brain tumor in childhood and is stratified into four molecular groups – Wingless and Int-1 (WNT), Sonic hedgehog (SHH), Group 3 and Group 4. Group 3 MB patients exhibit the poorest prognosis, with a 5-year overall survival of <60%, followed by Group 4 MB patients. Apart from MYC amplification in a subset of Group 3 MBs, the molecular pathomechanisms driving aggressiveness of these tumors remain incompletely characterized. The gene encoding the mTOR substrate and mRNA translation inhibitor eukaryotic translation initiation factor 4E-binding protein 1 (EIF4EBP1) represents a possible MYC target gene whose corresponding protein, 4EBP1, was shown to be more active in Group 3 versus Group 4 MBs. However, the prognostic role of 4EBP1 in MB and the mechanisms supporting 4EBP1 overexpression in Group 3 MB are still elusive. We analyzed EIF4EBP1 mRNA expression in publicly available data sets and found an upregulation in MB as compared to nonneoblastic brain. EIF4EBP1 mRNA expression levels were higher in Group 3 compared to Group 4 MBs. EIF4EBP1 mRNA expression was correlated with MYC expression, most prominently in Group 3 MBs. Survival analyses highlighted that high EIF4EBP1 mRNA expression was associated with reduced overall and event-free survival across all MB patients and in Group 3/Group 4 MB patients. Immunohistochemical evaluation of 4EBP1 protein expression in MB tissues confirmed that high levels of 4EBP1 are associated with poor outcome. Functional analyses revealed that MYC directly regulates EIF4EBP1 promoter activity, providing a mechanism for increased EIF4EBP1 mRNA levels in Group 3 MBs. Finally, we observed that 4EBP1 may support colony formation of in vitro cultured MB cells. Our data highlight that transcriptional upregulation of EIF4EBP1 by MYC promotes in vitro tumorigenicity of MB cells and associates with shorter survival of MB patients.

Cell Death Discovery (2025)11:330; https://doi.org/10.1038/s41420-025-02601-x

INTRODUCTION

Medulloblastoma (MB) is the most common malignant tumor of the central nervous system in children aged between 1-9 years [1]. MBs have been stratified into four distinct molecular groups, namely Wingless and Int-1 (WNT), Sonic Hedgehog (SHH), Group 3 and Group 4, that are driven by different molecular pathomechanisms and characterized by distinct DNA methylome and gene expression profiles [2]. These four MB groups have been incorporated in the World Health Organization (WHO) Classifications of Tumors of the Central Nervous System in 2016 [3] and in 2021 [4], with Group 3 and 4 MBs considered together as MBs without WNT and SHH activation (MBs, non-WNT/non-SHH). Each

MB group is associated with different prognosis, i.e., patients with WNT MBs have the best prognosis, with a survival rate of >95% beyond 5 years, as these tumors rarely present with metastatic spread at diagnosis and respond well to current therapy. SHH MB patients present with an intermediate to poor prognosis, depending on patient age, tumor histology, and metastatic status [5]. While survival of Group 4 MB patients is considered intermediate, Group 3 MB is the most aggressive MB group, characterized by a high incidence of cerebrospinal fluid (CSF) metastasis at diagnosis and displaying a 5-year overall survival of <60% [5]. The standard treatment of MBs consists of surgical resection followed by radiation and chemotherapy. Based on the

¹Institute of Neuropathology, University Hospital Düsseldorf and Medical Faculty, Heinrich Heine University, Düsseldorf, Germany. ²Department of Pediatric Oncology, Hematology, and Clinical Immunology, University Hospital Düsseldorf and Medical Faculty, Heinrich Heine University, Düsseldorf, Germany. ³Department of Molecular Oncology, British Columbia Cancer Research Centre, Vancouver, BC, Canada. ⁴Department of Pathology and Laboratory Medicine, University of British Columbia, Vancouver, BC, Canada. ⁵Department of Pathology, Mass General Brigham, Harvard Medical School, Boston 02114 MA, USA. ⁶German Cancer Consortium (DKTK), Partner site Essen/Düsseldorf, Düsseldorf, Germany. ⁷Department of Pediatric Oncology and Hematology, Saarland University Medical Center and Saarland University Faculty of Medicine, Homburg/Saar, Germany. ⁸Institute of Genetics, Heinrich Heine University, Düsseldorf, Germany. ⁹Institut Curie, Université Paris-Sud, Université Paris-Saclay, CNRS UMR 3347, INSERM U1021, Orsay, Paris, France. ¹⁰Department of Life Sciences, Faculty of Natural Sciences, Ben-Gurion University of the Negev, Beer-Sheva, Israel. ¹¹The National Institute for Biotechnology in the Negev, Ben-Gurion University of the Negev, Beer-Sheva, Israel. ¹²These authors contributed equally: Laura Hruby, Katerina Schaal. ^{Exp}email: gabriel.leprivier@med.uni-duesseldorf.de

Received: 29 July 2024 Revised: 28 May 2025 Accepted: 24 June 2025

Published online: 16 July 2025

MB group assignment and risk assessment, the radiation intensity is adapted and additional agents such as SHH inhibitors or novel agents are evaluated in clinical trials [5].

In contrast to SHH and WNT MBs, Group 3 and Group 4 MBs do not harbor frequent and well-defined genomic alterations [5]. Furthermore, the biological mechanisms underlying the difference in prognosis between Group 3 and Group 4 MB patients remain to be explained at the molecular level [6]. Certain high-risk factors, such as MYC amplification in Group 3 (17% of patients) or MYCN amplification in Group 4 (6% of patients) are recognized as important features [7], but the majority of patients in either group do not harbor these genetic alterations [7]. Further genomic analyses have been conducted to better delineate MB groupspecific features. Specifically, Group 3 and Group 4 MBs were each subdivided in three subgroups - namely alpha, beta and gamma [8]. Another study separated Group 3 and Group 4 MBs into eight molecular subtypes (I-VIII) by pairwise sample similarity analysis of DNA methylation profiles of a large MB patients cohort [7]. These analyses revealed that only certain subgroups or subtypes are characterized by MYC or MYCN amplification, which is associated with poor clinical outcome [7, 8]. In particular, only the Group 3 subgroup gamma exhibited a gain or an amplification of MYC [8], which was associated with the poorest overall survival among the Group 3 subgroups [8]. MYCN amplification was mainly detected in Group 4 subgroup alpha MBs [8]. In molecular subtypes as defined by Northcott et al., MYC amplification is more frequent in subtypes II and III, which include Group 3 MB patients only, and in subtype V, consisting mostly of Group 4 but also include Group 3 tumors [5, 7]. Stratification of Group 3 and Group 4 MB patients has been recently harmonized by analyzing a large number of MB patients, including patients of the Cavalli et al. cohort [9]. This highlighted the same eight subtypes as initially defined by Northcott et al. [7, 9], which are now incorporated as eight subgroups (I-VIII) in the 2021 WHO classification [4].

In mice, *MYC* overexpression, together with *Trp53* deletion, drives initiation and supports maintenance of MBs that resemble human Group 3 MBs [10, 11], highlighting the contribution of MYC to MB pathogenesis and aggressiveness. Paradoxically, *MYC* mRNA expression is also elevated in the WNT MBs group, to a similar level as in Group 3 MBs, which indicates that *MYC* expression – in contrast to *MYC* amplification – is not a reliable prognostic factor in MB patients [12]. As a transcription factor, MYC regulates the expression of numerous pro-tumorigenic genes [13]. One such MYC target gene, with potential clinical relevance in MBs, is the eukaryotic initiation factor 4E binding protein 1 (*EIF4EBP1*) [14, 15].

EIF4EBP1 encodes the mRNA translation inhibitor 4EBP1, which is directly regulated by the energy-sensing mechanistic target of rapamycin complex 1 (mTORC1) [16]. While under normal conditions, 4EBP1 is phosphorylated and blocked by mTORC1, 4EBP1 gets activated under metabolic stress conditions following mTORC1 inhibition, and thus binds and blocks the mRNA translation initiation factor eIF4E, leading to inhibition of mRNA translation initiation [17, 18]. While 4EBP1 appears to exert tumor suppressor activity, since it blocks the oncoprotein elF4E [19], inhibits cellular proliferation [20] and restricts tumor growth in genetically engineered mouse models of prostate [21] as well as head and neck squamous cell carcinoma (HNSCC) [22], protumorigenic functions also have been reported for 4EBP1. Indeed, it was reported that 4EBP1 promotes angiogenesis in ovarian and breast cancer models, thereby facilitating tumor growth under hypoxia [23, 24], supports oncogenic transformation [25, 26], and promotes glioma and Ewing sarcoma tumorigenicity [25, 27]. However, the role of 4EBP1 in MBs is currently unknown.

EIF4EBP1 mRNA expression is upregulated in numerous tumor entities [25, 28] and high EIF4EBP1 mRNA levels correlate with poor survival in several cancer types [14, 25, 27–33]. In MBs, the amount of phosphorylated 4EBP1, i.e., inactive 4EBP1, was reported to be lower in non-SHH/non-WNT MBs when compared

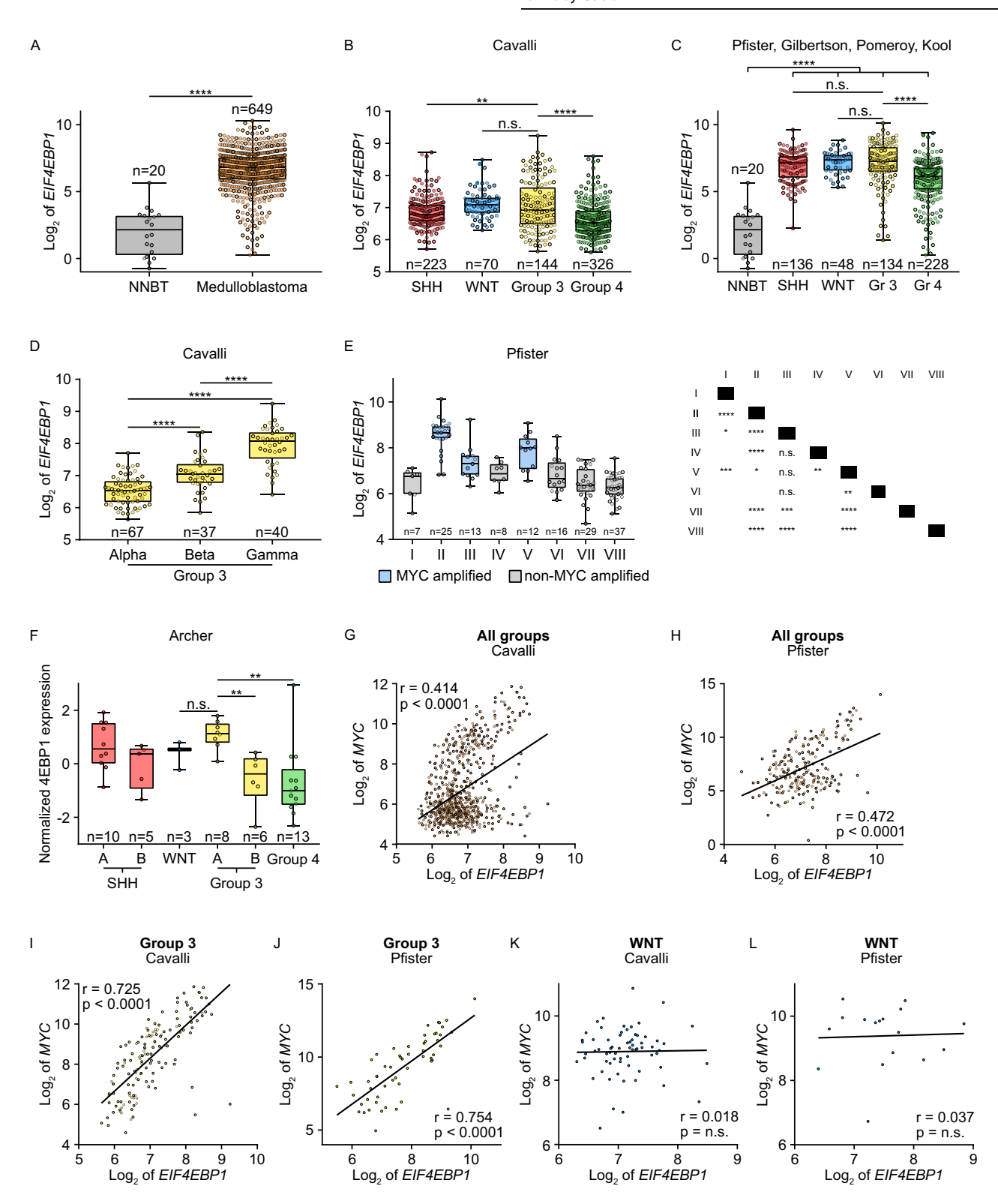
to SHH and WNT MBs [34]. In another study, 4EBP1 protein levels were found to be higher in Group 3 versus Group 4 MBs without any changes in phosphorylated 4EBP1 levels [35], thus suggesting that 4EBP1 is more active in Group 3 MBs. However, it is currently unknown whether *EIF4EBP1* mRNA and 4EBP1 protein expression are associated with patient outcome in MBs and what the drivers of 4EBP1 overexpression in Group 3 MBs are. So far, only a few transcription factors have been characterized to promote *EIF4EBP1* transcription in other tumor entities, including the androgen receptor in prostate cancer [36], ETS1 and MYBL2 in glioblastoma [37], and MYCN in neuroblastoma [29]. Additionally, MYC was shown to directly control *EIF4EBP1* transcription in colon adenocarcinoma [14] and prostate cancer cells [15], supporting that *EIF4EBP1* represents a MYC target gene.

Here, we analyzed the mRNA expression of *EIF4EBP1* in MB groups and subgroups using several publicly available MB expression data sets, and assessed its potential association with *MYC* mRNA expression levels and *MYC* gene amplification status. We determined the prognostic role of *EIF4EBP1* mRNA expression in MB patients and examined 4EBP1 protein expression as a prognostic biomarker in an institutional MB patient cohort. Using functional assays, we delineated the regulation of *EIF4EBP1* transcription by MYC in MB cells and characterized the contribution of 4EBP1 to clonogenic growth of MB cells in vitro.

RESULTS EIF4EBP1 mRNA levels are elevated in MBs

To investigate *EIF4EBP1* mRNA expression in MB tissues, we pooled and analyzed publicly available data from two non-neoblastic brain and seven independent and non-overlapping MB datasets. We found that *EIF4EBP1* mRNA expression was significantly upregulated in MB tissues compared to non-neoplastic brain tissues (Fig. 1A). This was not related to a hypomethylation of *EIF4EBP1* promoter region, as DNA methylation levels of 18 CpG sites within the *EIF4EBP1* promoter region (hg19; Chr8: 37,886,955-37,917,868) were not different in normal pediatric brain tissues versus MB tumor tissues (Supplementary Fig. 1A). Assessing the association of *EIF4EBP1* mRNA expression with MB risk factors revealed that *EIF4EBP1* mRNA levels were higher in relapsed versus primary MB tissues (Supplementary Fig. 1B), while *EIF4EBP1* mRNA expression was similar in metastatic versus primary MB tissues (Supplementary Fig. 1C, D).

Analysis of EIF4EBP1 mRNA expression levels according to MB groups showed, in two single patient cohorts [8, 38] as well as in a pooled patient cohort [7, 39-41], that EIF4EBP1 mRNA expression was elevated in Group 3 relative to Group 4 MBs (Fig. 1B, C; Supplementary Fig. 1E; Table S8), in accordance to previous observations made for 4EBP1 protein levels using proteomics data [35]. However, EIF4EBP1 mRNA levels were as high in WNT MBs, the least aggressive MBs group, as in Group 3 MBs (Fig. 1B, C; Table S7). While EIF4EBP1 was more strongly expressed in Group 3 compared to SHH MBs in the Cavalli et al. MBs cohort [8] (Fig. 1B), this difference was not obvious in pooled datasets [7, 39-41] (Fig. 1C). We next investigated levels of EIF4EBP1 mRNA expression according to Group 3 and Group 4 subgroups as defined by Cavalli et al. [8] and by Northcott et al. (Pfister cohort) [7]. This highlighted that in Group 3, EIF4EBP1 was more highly expressed in the gamma subgroup, the most aggressive Group 3 subgroup (corresponding mainly to subtype II [42]), as compared to alpha and beta subgroups, while in Group 4, EIF4EBP1 levels were higher in the alpha subgroup (corresponding to subtypes V and VI [42]) compared to the other subgroups (Fig. 1D and Supplementary Fig. 1F). Noteworthy, MYC gain or amplification is a feature of Group 3 subgroup gamma, while MYCN amplification is a characteristic of Group 4 subgroup alpha [8], thus pointing to a relationship between high EIF4EBP1 expression and MYC(N) amplification in MBs. In line with that, we uncovered in the Pfister cohort [7] that EIF4EBP1 expression is most elevated in



subtypes II, III and V, which are characterized by MYC amplification (20% of cases for subtype II and 10% of cases for subtypes III and V [7]) (Fig. 1E). Using proteomic data extracted from the Archer et al. dataset [43], we confirmed that consistently with EIF4EBP1 mRNA expression, 4EBP1 protein expression was significantly higher in Group 3A, corresponding to subtype II [7], as compared to Group 4 and Group 3B but was at the same level than in the WNT subgroup (Fig. 1F).

Finally, we assessed *EIF4EBP1* copy number alterations in Cavalli et al. [8] Group 3 and Group 4 MBs as a possible mechanism supporting *EIF4EBP1* overexpression. We observed a high frequency of *EIF4EBP1* gain in Group 3 subgroup gamma (corresponding mainly to subtype II [42]) (50% of cases), which was not the case in the other Group 3 subgroups (Supplementary Fig. 1G). In contrast, only around 2% of Group 4 subgroup alpha (corresponding to subtypes V and VI [42]) showed *EIF4EBP1* gain

Fig. 1 *EIF4EBP1* mRNA is upregulated and is co-expressed with *MYC* in MBs. A Expression levels of *EIF4EBP1* mRNA in a pool of non-neoplastic brain tissues (NNBT) (Roth et al. (n = 9) [63] and Pomeroy et al. (n = 11) [40] cohorts) compared to a pool of MB tissues (denBoer (n = 27) [64], Delattre (n = 54), Gilbertson (n = 73) [39], Hsieh (n = 22) [65], Kool et al. (n = 62) [41], Pfister (n = 223) [7] and Pomeroy (n = 188) [40] cohorts). **B, C** Expression levels of *EIF4EBP1* mRNA according to the four MB groups SHH, WNT, Group 3 and Group 4 using the Cavalli et al. cohort [8] or a pool of the Kool et al., Gilbertson, Pfister and Pomeroy cohorts [7, 39–41] compared to a pool of non-neoplastic brain tissue (NNBT) (Roth et al. [63] and Pomeroy et al. [40] cohorts) (see Table S2 for the number of patient samples per group and Table S7 for the results of pair-wise statistic tests between different groups). **D** Expression levels of *EIF4EBP1* mRNA according to subgroups of Group 3 MBs from the Cavalli et al. cohort [8]. **E** Expression levels of *EIF4EBP1* mRNA according to the Heidelberg subtypes from the Pfister cohort [7]. Significance in (A–E) was calculated using an unpaired and two-tailed parametric t test (*t0.001, **t0.001, **t0.001, **t0.001, **t0.0001, **t0.000

Table 1. GSEA of MYC-upregulated genes co-expressed with $\it ElF4EBP1$ in MB groups.

| Group | p value | Number of genes |
|---------|---------|-----------------|
| SHH | 6.2e-11 | 16 |
| WNT | 0.03 | 5 |
| Group 3 | 4.8e-45 | 56 |
| Group 4 | 0.03 | 3 |

Broad institute: MYC_UP.V1_UP; cut-off: r = 0.45.

(Supplementary Fig. 1H), indicating that levels of *EIF4EBP1* expression are impacted by copy number alterations in Group 3 MB but not in Group 4 MB subgroups.

In conclusion, *EIF4EBP1* mRNA and 4EBP1 protein expression are increased in MBs, particularly in the most aggressive subgroups characterized by *MYC* or *MYCN* gene amplification.

EIF4EBP1 expression is associated with MYC expression in MBs

To elucidate the possible link between EIF4EBP1 and MYC mRNA expression in MBs, we analyzed their expression levels in the different MB groups of the Cavalli et al. [8] and Pfister [7] cohorts. We found that EIF4EBP1 and MYC mRNA levels were strongly associated with each other across all MB patients ([r] 0.414, p value < 0.0001; Fig. 1G; [r] 0.472, p value < 0.0001; Fig. 1H). Correlative analyses according to MB groups showed in Group 3 an even stronger correlation between EIF4EBP1 and MYC mRNA expression ([r] 0.725, p value < 0.0001; Fig. 1I; [r] 0.754, p value < 0.0001; Fig. 1J). In Group 4 MBs, EIF4EBP1 mRNA expression was not correlated with MYC mRNA expression ([r] 0.118, p value < 0.01; Supplementary Fig. 11; [r] 0.194, p value = n.s.; Supplementary Fig. 1J), but strongly associated with MYCN mRNA expression ([r] 0.534, p value < 0.0001; Supplementary Fig. 1K; [r] 0.507, p value < 0.0001; Supplementary Fig. 1L), consistent with MYCN amplification being a common hallmark feature of this MB group [5]. Further analyses indicated that MYCN mRNA levels neither correlated positively with EIF4EBP1 mRNA levels across all MB groups ([r] 0.220, p value < 0.0001; Supplementary Fig. 2A; [r] 0.087, p value = n.s.; Supplementary Fig. 2B) nor in Group 3 MBs ([r] -0.199, p value < 0.05; Supplementary Fig. 2C; [r] -0.468, p value < 0.001; Supplementary Fig. 2D).

There was no significant association between mRNA levels of $\it EIF4EBP1$ and $\it MYC$ in the WNT MBs group ([r] 0.018, $\it p$ value = n.s.; Fig. 1K; [r] 0.037, $\it p$ value = n.s.; Fig. 1L), even though this group displayed high $\it MYC$ mRNA expression levels in the analyzed cohorts [12]. Moreover, only five MYC target genes (as defined from the human gene set "Broad institute: MYC_UP.V1_UP" [44]) were significantly co-expressed with $\it EIF4EBP1$ in WNT MBs as opposed to 56 MYC target genes in Group 3 MBs (Table 1). These data are in accordance with the findings of Forget et al. [35], namely that MYC

activity is lower in WNT MBs than in Group 3 MBs despite similar levels of MYC transcripts. Further analysis of the Cavalli et al. [8] and Pfister [7] cohorts highlighted highly significant associations between EIF4EBP1 and MYC mRNA levels in the MYC-amplified MB subgroups, namely Group 3 subgroup gamma (corresponding mainly to subtype II [42]) ([r] 0.704, p value < 0.0001; Supplementary Fig. 2E) and subtypes II, III and V combined ([r] 0.604, p value < 0.0001; Supplementary Fig. 2F), confirming co-expression of EIF4EBP1 and MYC in MYC-driven MB tissues.

High EIF4EBP1 mRNA expression is associated with shorter survival of MB patients

We next determined whether EIF4EBP1 mRNA expression is linked to prognosis of MB patients. To do so, we analyzed two independent and non-overlapping MB patient cohorts, i.e., Cavalli et al. [8] and Pomeroy [40] cohorts. Kaplan Meier estimates revealed that high EIF4EBP1 mRNA levels (using first versus last quartile of expression level as cut-off) was significantly associated with reduced overall survival across all MB groups in both cohorts (p value = 0.013; Fig. 2A; p value = 9.3e⁻⁰³; Fig. 2B). When restricting our analyses to the most aggressive cases, focusing on Group 3 and Group 4 patients combined, we uncovered that high EIF4EBP1 expression was similarly associated with poor outcome in both cohorts (p value = $2.8e^{-03}$; Fig. 2C; p value = $7.9e^{-03}$; Fig. 2D). However, in the same cohorts there was no significant association between EIF4EBP1 mRNA levels and overall survival in Group 4 MB patients only (p value = 0.096; Supplementary Fig. 3A; p value = 0.184; Supplementary Fig. 3B). This is in contrast with the association we observed between high EIF4EBP1 expression and unfavorable outcome in Group 3 MB patients of the Cavalli et al. cohort [8] (p value = 0.025; Fig. 2E). Further analyses indicate that EIF4EBP1 mRNA expression levels were not correlated to overall survival in the WNT MBs group (p value = 1.000; Fig. 2F) and the SHH MBs group (p value = 0.272; Supplementary Fig. 3C) of the Cavalli et al. cohort [8]. However, EIF4EBP1 expression could not be analyzed using the Pomeroy et al. cohort [40] for the Group 3, WNT or SHH MB groups separately as patient numbers were too low. These data suggest that high EIF4EBP1 expression are linked to less favorable prognosis across all MB patients as well as in Group 3 MB patients.

High 4EBP1 protein expression is associated with unfavorable prognosis of MB patients

Since mRNA expression is not strongly correlated with protein expression in MBs (Spearman correlation coefficient of 0.53 [35]), we interrogated the prognostic value of 4EBP1 protein expression in this tumor entity. Using a previously established anti-4EBP1 antibody [29], we immunostained FFPE tissue sections from an institutional MB cohort consisting of 61 tumors from all groups, as described previously [45, 46] (Fig. 3A, B). Immunostaining for 4EBP1 was both cytoplasmic and nuclear, consistent with previous reports [47, 48] (Fig. 3B). In line with our observations

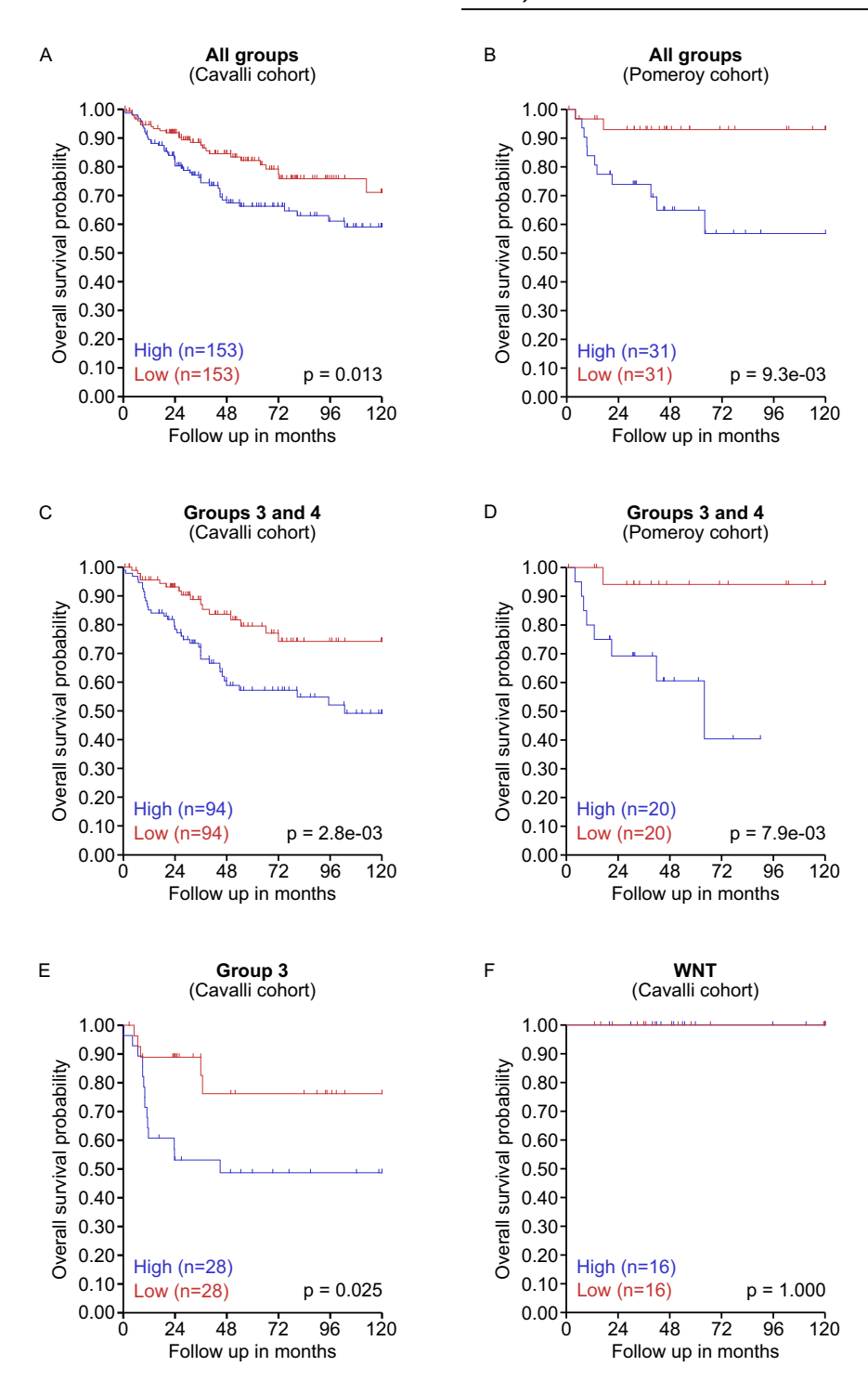
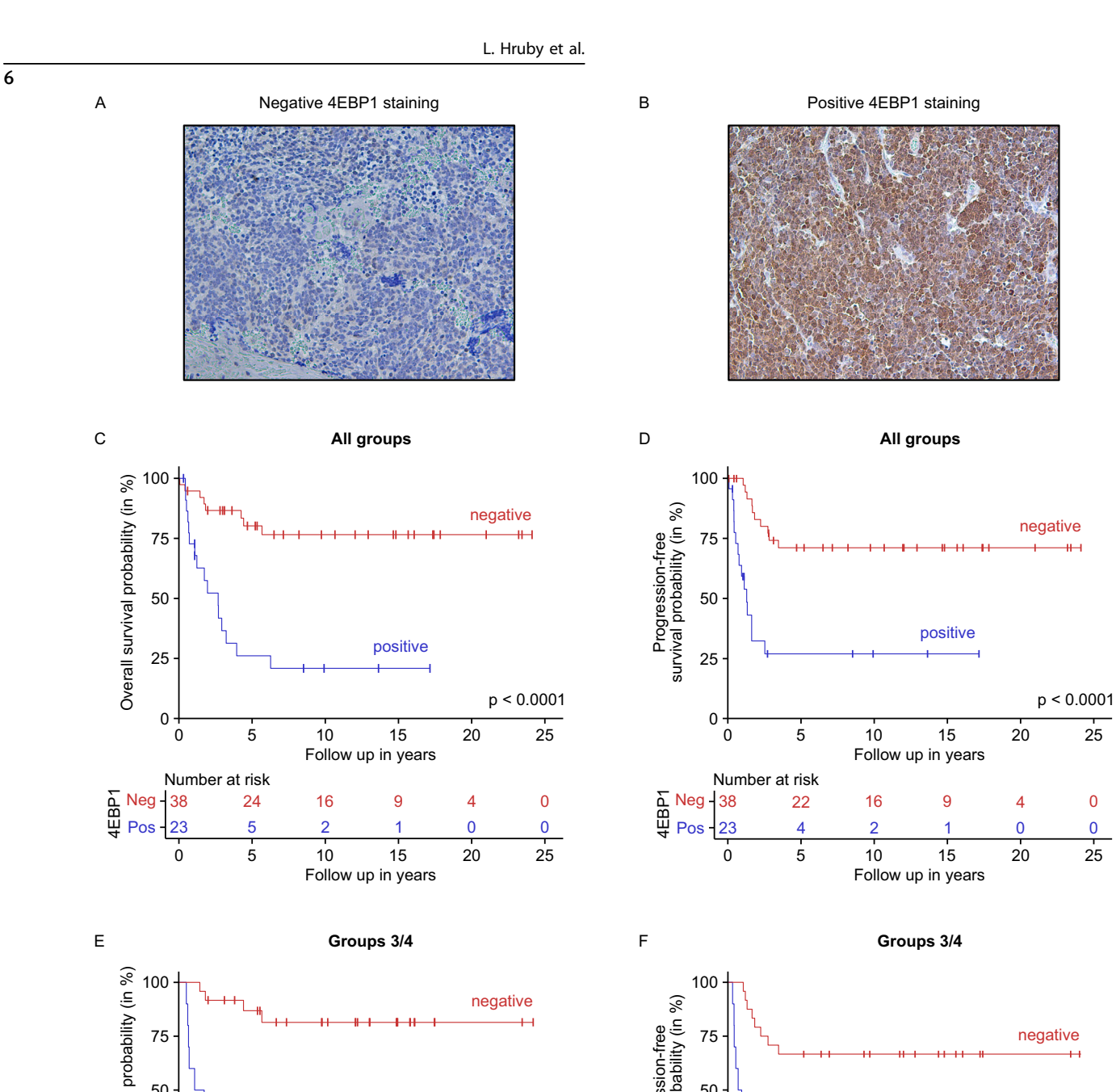


Fig. 2 *EIF4EBP1* mRNA expression correlates with overall survival in all MB patients and in Group 3/Group 4 MB patients. A–F Kaplan–Meier survival estimates of overall survival of MB patients stratified by their *EIF4EBP1* mRNA expression levels across all MB patients (**A**, **B**), in Group 3 and 4 MB patients combined (**C**, **D**), in Group 3 MB patients (**E**) or in WNT MB patients (**F**) using data sets from the Cavalli et al. [8] and Pomeroy [40] cohorts as indicated. The data were obtained from R2 Genomics and visualization platform and the first versus last quartile was used as cut-off. Significance was calculated with the log-rank test.

on *EIF4EBP1* mRNA expression (Supplementary Fig. 1B), we confirmed that 4EBP1 protein levels were higher in relapsed compared to primary MB tissues (Supplementary Fig. 4A). Kaplan–Meier analysis showed that positive 4EBP1 staining was strongly associated with reduced overall and progression-free survival across the entire MB cohort (*p* value < 0.0001; Fig. 3C; *p* value < 0.0001; Fig. 3D). Additionally, we uncovered that

4EBP1 staining was positively associated with poor overall and progression-free survival in the subset of patients with Group 3 and Group 4 MB (p value < 0.0001; Fig. 3E; p value = 0.00023; Fig. 3F). Due to the limited number of cases, such correlation could not be determined separately for Group 3 MB patients alone. Representative immunostaining for 4EBP1 in each MB subgroup is displayed in Supplementary Fig. 4B.



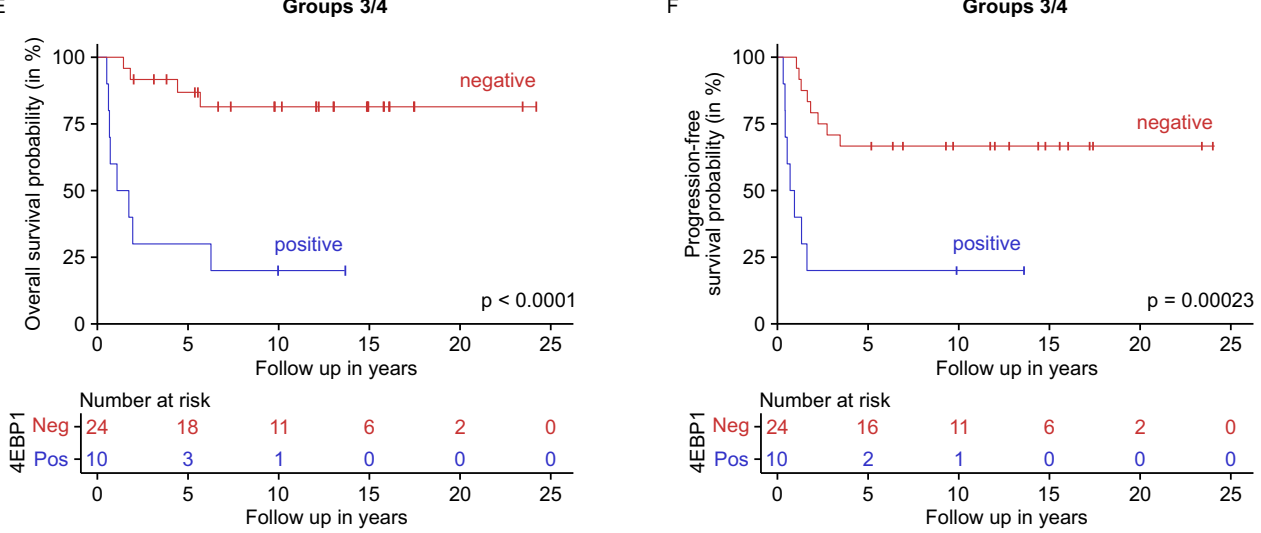
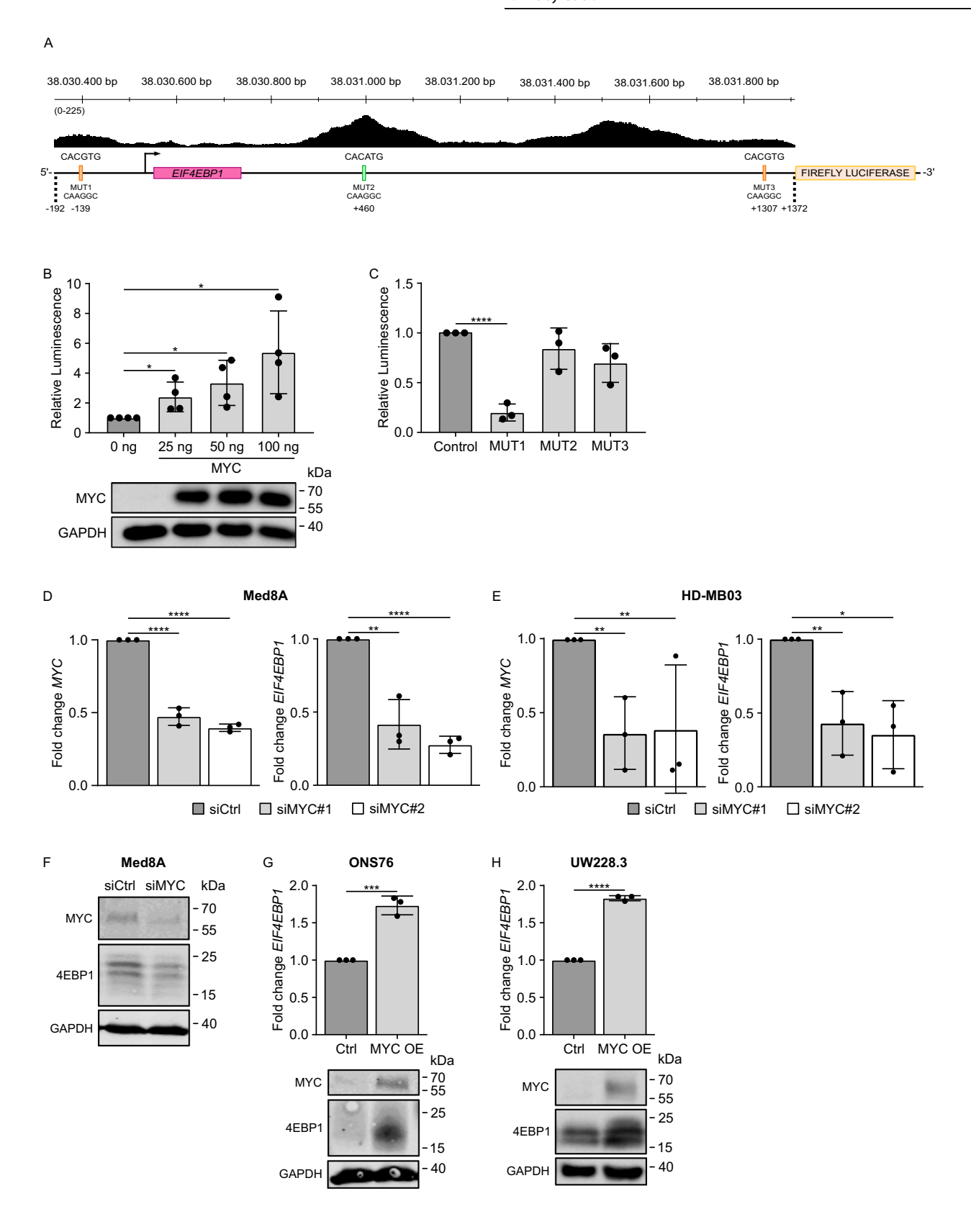


Fig. 3 High 4EBP1 protein expression is associated with unfavorable prognosis of MB patients. A, B Representative images of negative (A) and positive (B) 4EBP1 immunohistochemical staining of selected MB samples represented on the MBs TMA. C–F Kaplan–Meier survival estimates of overall survival (C, E) or progression free-survival (D, F) of MB patients stratified by their 4EBP1 staining score in all patients (C, D) or in Group 3 and Group 4 combined (E, F).



 $\it EIF4EBP1$ expression is regulated at the transcriptional level by MYC in MBs

As we uncovered an association between *EIF4EBP1* and *MYC* mRNA expression in MB tissues, and since MYC has been described to control *EIF4EBP1* transcription in other tumor types [14, 15], we asked

whether *EIF4EBP1* also represents a MYC target gene in MBs. This could provide a molecular mechanism for the *EIF4EBP1* overexpression we observed in the most aggressive MB groups (see Fig. 1).

We initially analyzed available chromatin immunoprecipitation (ChIP)-sequencing (seq) data from the Encode Consortium, which

Fig. 4 MYC activates EIF4EBP1 promoter activity and transcription in MBs. A ChIP peak locations within the human EIF4EBP1 promoter, exon 1 and part of intron 1 (hg38; Chr8: 38,030,342 - 38,031,906) from ChIP-sequencing data for MYC (Encode consortium, Encyclopedia of DNA Elements at UCSC [57, 58]) and an illustration of the luciferase reporter construct containing the EIF4EBP1 promoter, exon 1 and part of intron 1 (-192; +1372) coupled to Firefly luciferase, with the indicated binding sites of the transcription factor MYC. The three E boxes present in the promoter, and corresponding introduced mutations, are indicated. \vec{B} , C HEK293-T cells were transfected with the (-192; +1372) EIF4EBP1 promoter reporter construct, together with 25 ng, 50 ng and 100 ng MYC (B) or the (-192; +1372) EIF4EBP1 promoter reporter constructs containing a mutation of each of the E boxes (as indicated in A), together with 25 ng MYC (C). For (B) and (C), a Renilla Luciferase vector was used as an internal control and luciferase activities were detected using the Dual-Luciferase Reporter Assay. Firefly luciferase activity was normalized to Renilla luciferase activity and the ratio was normalized to the corresponding 0 ng (B) or control (C) condition. Data represent the mean of four (B) or three (C) independent replicates ± standard deviation (SD). Significance was calculated using an unpaired and two-tailed parametric t test (*p < 0.05, ****p < 0.0001). A representative immunoblot analyzing expression of MYC is presented in (**B**). D, E Med8A (D) and HD-MB03 (E) MB cells were transiently transfected with negative control siRNAs (siCtrl), or two different siRNAs each targeting MYC (siMYC#1 and siMYC#2). Cells were re-transfected after 96 h with their corresponding siRNA and incubated for a total of 168 h. MRNA was harvested to determine the expression levels of EIF4EBP1 and MYC by qRT-PCR. Data obtained by qRT-PCR represent the mean of three independent replicates ± SD and the fold change in expression was normalized to the negative control (siCtrl). Significance was calculated using an unpaired and two-tailed parametric t test (*p < 0.05, **p < 0.01, ****p < 0.0001). **F** Med8A MB cells were transiently transfected with negative control (siCtrl) or a pool of four different siRNAs (see Table S5) targeting MYC (siMYC). Cells were incubated 72 h and protein was harvested for immunoblotting using the indicated antibodies. G, H Control and MYC overexpressing (MYC OE) ONS76 (G) or UW228.3 (H) cells were lysed. Levels of EIF4EBP1 mRNA were determined by qRT-PCR. Levels of 4EBP1 and MYC proteins were determined by immunoblots using the indicated antibodies. Data obtained by gRT-PCR represent the mean of three independent replicates ± SD and the fold change in expression was normalized to the control. Significance was calculated using an unpaired and two-tailed parametric t test (***p < 0.001, ****p < 0.0001).

demonstrated direct binding of MYC at three positions within the EIF4EBP1 transcriptional regulatory region (encompassing the promoter region, exon 1 and intron 1) (Fig. 4A). This was detected in various normal and cancer cells, however, not including MBs or any type of brain cancer cells (Table S3). In accordance with previous studies [14, 15], we confirmed the presence of three E boxes, i.e. MYC-binding sites, within this region, including two consensus motifs (CACGTG) and one non-canonical motif (CACATG) (Fig. 4A). Using a luciferase reporter assay containing the nucleotides –192 to +1372 of the EIF4EBP1 promoter region, exon 1, and part of intron 1 (Fig. 4A), which contains the three ChIP peaks for MYC, we demonstrated that MYC overexpression dose-dependently activated the EIF4EBP1 promoter in HEK293-T cells (Fig. 4B). To delineate which of the three E boxes is/are necessary for the transcriptional regulation of the EIF4EBP1 promoter by MYC, we mutated separately each of the E boxes located within the -192 to +1372 EIF4EBP1 reporter, as indicated in Fig. 4A. Mutation of only E box 1 compromised MYC-mediated activation of EIF4EBP1 promoter (Fig. 4C), in contrast to the involvement of the three E boxes for MYCN regulation of EIF4EBP1 promoter activity as previously reported [29]. These data support that MYC regulates EIF4EBP1 promoter activity primarily through one specific E box (E box 1), even though it binds three E boxes within this transcriptional regulatory region.

To determine whether MYC is regulating EIF4EBP1 mRNA expression in MBs, we transiently knocked down (KD) MYC in two different MYC-amplified MB cell lines, namely Med8A and HD-MB03, and measured EIF4EBP1 mRNA expression. Upon MYC KD, both MYC and EIF4EBP1 mRNA levels decreased significantly in both cell lines (Fig. 4D, E). This was associated with a reduction of 4EBP1 protein levels in Med8A (Fig. 4F). Functionally, MYC KD led to a marginal increase of cell death and a slight decrease of the proliferation rate, as expected (Supplementary Fig. 5A, B). To further validate the regulation of EIF4EBP1/4EBP1 expression by MYC in MB cells, we used stable MYC overexpression models established in two MB cell lines harboring low MYC levels, namely ONS76 and UW228.3 [49]. We observed increased EIF4EBP1 mRNA levels in both MYC overexpressing ONS76 and UW228.3 cells, compared to the corresponding control cells (Fig. 4F, G). Moreover, MYC overexpression resulted in increased 4EBP1 protein levels in both cell lines (Fig. 4H, I). Taken together, these data support that MYC regulates EIF4EBP1 transcription in MBs by directly regulating its promoter activity.

4EBP1 contributes to tumorigenic potential of MB cells

Given the clinical relevance we uncovered for *EIF4EBP1* mRNA and 4EBP1 protein expression in MB patients, we wondered whether

4EBP1 contributes to cell migration and exerts a pro-tumorigenic function in this tumor entity, as reported in gliomas [25] and Ewing sarcomas [27]. Furthermore, we previously reported that 4EBP1 promotes the survival of MB cells under glucose starvation [25], a feature that has been linked to tumorigenic promotion [50]. To investigate the potential tumor-supportive function of 4EBP1 in MB cell models, we investigated HD-MB03 and Med8A cells upon inducible 4EBP1 KD using either a migration assay or soft agar colony formation assays. KD of 4EBP1 using two different shRNAs, as validated by immunoblot, had no effect on migratory properties (Supplementary Fig. 6A, B) but resulted in decreased colony formation of approximately 23% in both MB cell lines when compared to the corresponding shRNA controls (Fig. 5A, B). We also assessed the effect of 4EBP1 KD on additional cell properties, such as energy levels and proliferation. Energy levels were slightly higher in the 4EBP1 KD cell lines as compared to controls (Supplementary Fig. 6C, D), whereas proliferation rates were not affected by 4EBP1 KD in both MB cell lines (Fig. 5C, D). This indicates that 4EBP1 contributes to the tumorigenic potential of MYC-amplified MB cells independently of growth rate.

DISCUSSION

We report here that mRNA expression of the mTORC1 substrate and mRNA translational repressor EIF4EBP1 is increased in MBs, as compared to non-neoblastic brain tissue, is higher in Group 3 versus Group 4 MBs, and is associated with patient outcome. This is reminiscent of another negative regulator of mRNA translation, namely EEF2K, whose expression in MBs was reported to demonstrate the same features [51], suggesting a high level of translational regulation in Group 3 MBs. In line with that, proteomics analysis revealed that a number of mRNA translation initiation factors, as well as 4EBP1, are overexpressed in Group 3 versus Group 4 MBs [35]. The activity of 4EBP1 is not only dependent on its protein level but also on its phosphorylation states, which is a result of mTORC1 activity [17, 18]. Noteworthy, it was reported that levels of phospho-4EBP1, indicative of inactive 4EBP1, are higher in WNT and SHH as compared to non WNT/non SHH MBs [34]. Additionally, levels of phospho-4EBP1 were similar in Group 3 and Group 4 MBs, while expression of total 4EBP1 protein was higher in Group 3 versus Group 4 MBs [35]. These observations support that 4EBP1 activity is higher in Group 3 MBs compared to other MB groups, likely as a consequence of reduced mTORC1 activity in this MBs group. Together with our finding that 4EBP1 protein levels correlate with poor outcome across all MB

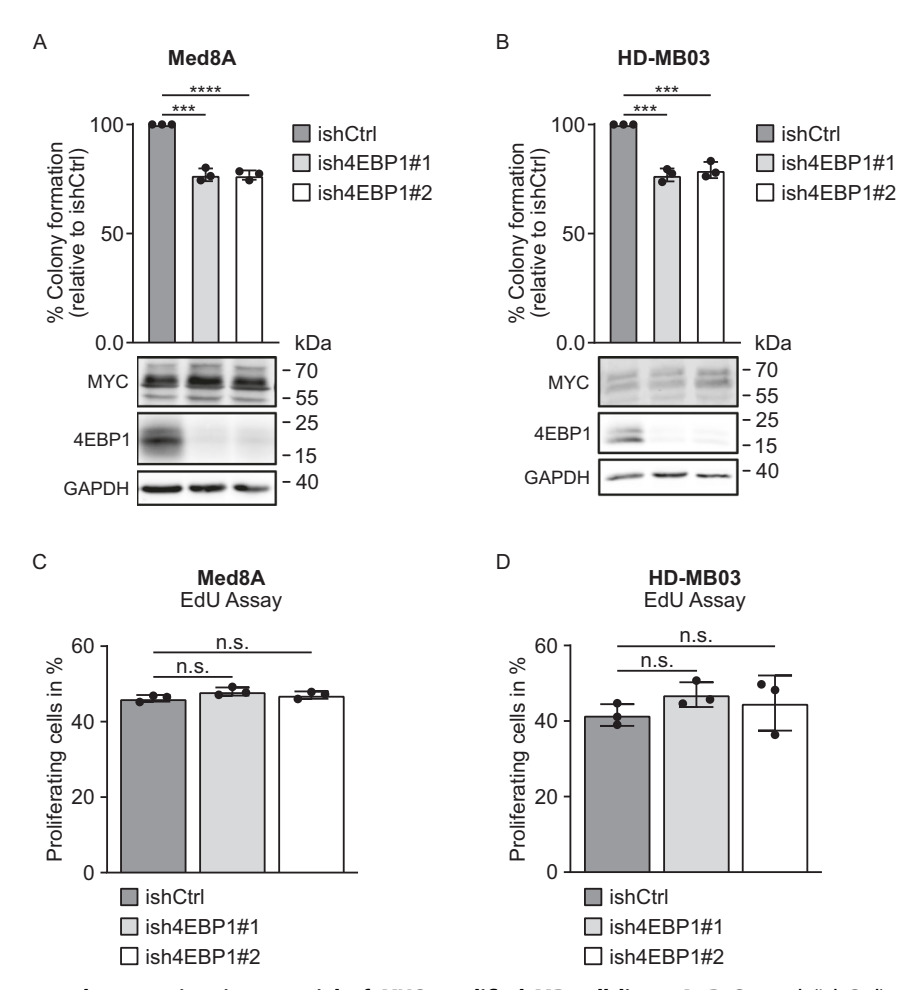


Fig. 5 4EBP1 contributes to the tumorigenic potential of MYC-amplified MB cell lines. A, B Control (ishCtrl) or stable inducible 4EBP1 knockdown (ish4EBP1#1 and #2) Med8A (A) or HD-MB03 (B) cells were treated with 1 μ g/ml doxycycline and grown in soft agar for 21 days. Colonies and single cells were counted, and colony formation efficiency was calculated and normalized to control. Data are reported as means \pm SD of three individual replicates with indicated significance. Protein expression of MYC and 4EBP1 was analyzed by immunoblotting. Significance was calculated using an unpaired and two-tailed parametric t test (***p < 0.001, ****p < 0.0001). C, D Control (ishCtrl) or stable inducible 4EBP1 knock down (ish4EBP1#1 and #2) Med8A (C) or HD-MB03 (D) were treated with 1 μ g/ml doxycycline and cell proliferation was measured with an EdU assay. Data are reported as means \pm SD of three individual replicates. Statistics were calculated using an unpaired and two-tailed parametric t test (n.s. = not significant).

groups as well as in Group 3/Group 4 MB patients, the available data highlight that *EIF4EBP1* mRNA and 4EBP1 protein expression may represent novel prognostic factors and possible biomarkers in MPs.

Amplifications of MYC or MYCN are well-known genetic alterations associated with higher risk MBs [7]. We report that EIF4EBP1 mRNA expression is associated with MYC mRNA expression in MBs, an association we found to be particularly evident in Group 3 MBs that are characterized by MYC gene amplification [7]. In line with that, we observed that EIF4EBP1 mRNA expression in Group 4 MBs is associated with elevated MYCN mRNA expression, as we previously reported in neuroblastoma [29]. Intriguingly, there was no association between EIF4EBP1 and MYC mRNA levels in WNT MBs. Furthermore, we found fewer MYC target genes to be co-expressed with EIF4EBP1 in WNT MBs compared to Group 3 MBs, which could reflect differences in MYC activity between the two groups. Interestingly, RNA profiling and proteomics analysis revealed that MYC target genes are highly overexpressed in Group 3 but not in WNT [35], despite similar levels of MYC expression in these groups, pointing to a differential activity of MYC in Group 3 versus WNT MBs. One may speculate that transcription factors other than MYC may contribute to EIF4EBP1 upregulation in WNT MBs, the identity of which remains to be unveiled. Noteworthy, phosphoproteomics data highlighted that MYC phosphorylation as indicator of active MYC is higher in Group 3A MBs – corresponding to subtype II [7] – versus Group 3B and Group 4 MBs [43]. Remarkably, we also uncovered that 4EBP1 protein is more highly expressed in Group 3A MBs compared to Group 3B and Group 4 MBs, further pointing to a link between MYC activity and *EIF4EBP1* mRNA and 4EBP1 protein expression in MRs

Our data indicate that the basis for the MYC and EIF4EBP1 coexpression relies on the transcriptional regulation of EIF4EBP1 by MYC in MB cells. While it was characterized by ChIP that EIF4EBP1 is a MYC target gene [14, 15], albeit not in MB cells, it has been elusive whether MYC regulates the EIF4EBP1 promoter. Here, we provide evidence that MYC activates the EIF4EBP1 promoter via one E box among the three E boxes previously characterized to be bound by MYC [14]. Additionally, we demonstrated that MYC induces EIF4EBP1 transcription in MB cell lines as knock down or overexpression of MYC decreased or increased EIF4EBP1 mRNA levels, respectively. This expands previous studies reporting on the control of EIF4EBP1 transcription by MYC in colorectal and prostate cancer cells [14, 15].

The function of 4EBP1 in cancer is still under debate as it can exert tumor suppressive or pro-tumorigenic functions [16],

depending on the tumor entity and the metabolic conditions of the tumor microenvironment. For instance, 4EBP1 was shown to mediate cell survival in response to hypoxia and induce angiogenesis in breast cancer models [23]. Furthermore, our previous findings highlighted that 4EBP1 promotes survival of cancer cells, including MB cells, under glucose starvation [25]. As glucose levels are particularly low in MBs as compared to other pediatric brain cancers [52], high 4EBP1 expression may confer resistance to MB cells against such metabolic stress conditions. Since molecular mechanisms of tumor adaptation to glucose starvation are similar to the ones promoting tumorigenesis [25, 50], and since we and others reported that 4EBP1 promotes tumorigenesis of glioblastoma and Ewing's sarcoma cells in vivo [25, 27], we explored 4EBP1 function in MB cells growth in vitro. Our findings suggest that 4EBP1 contributes to the tumorigenic capacity, i.e. clonogenic growth in soft agar, of MB cells in vitro, albeit to a moderate extent as 4EBP1 knock-down only restrained the clonogenic potential of the investigated MB cells by 20-25%. This could potentially be due to the lack of p53 activity in Med8A and HD-MB03 MB cells, which was reported for Med8A [53], as the pro-tumorigenic properties of 4EBP1 rely on the presence of an intact, active p53 as reported in oncogenic RAS transformed fibroblast models [26]. Noteworthy, the direct protein target of 4EBP1, eIF4E, is a well-known oncoprotein that was shown to promote MBs tumorigenesis [54]. Genetic inhibition of eIF4E suppressed MYCN-driven MB development in a genetically engineered mouse model of MBs [54]. While this may seem in apparent contradiction with the proposed function of 4EBP1 in MBs, it likely reflects the importance of the metabolic conditions within the MBs tumor microenvironment. As reported in mouse models of pancreatic cancer and glioblastoma, in well-perfused tumor areas, mTOR and eIF4E are active and their inhibition restricts tumor growth [55, 56]. In contrast, in poorly vascularized tumor areas, mTOR and eIF4E are inactive, while 4EBP1 is activated, which thus facilitates tumor cell survival and favors tumor growth in the long term [55, 56].

Taken together, our findings revealed that elevated *EIF4EBP1* mRNA and 4EBP1 protein expression are associated with shorter survival of MB patients. Increased *EIF4EBP1* mRNA and 4EBP1 protein expression is driven by MYC through direct binding to the *EIF4EBP1* promoter and activation of *EIF4EBP1* transcription, which in turn may contribute to higher clonogenic growth properties of MB cells in vitro and possibly more aggressive MBs behavior in patients.

MATERIALS AND METHODS

Data availability and bioinformatics analysis

We obtained *EIF4EBP1* mRNA expression, co-expression and survival data from publicly available non-neoplastic brain tissue and MB data sets from the R^2 Genomic Analysis Visualization Platform (R^2 AMC; http://r2.amc.nl). An overview of the used data sets and the corresponding GSE numbers is provided in Table S1. The number of patients per MB group in each cohort is listed in Table S2. For co-expression analyses of *EIF4EBP1* mRNA expression and *MYC* or *MYCN* mRNA expression, the Cavalli et al. [8] and Pfister [7] cohorts were used. *EIF4EBP1* mRNA expression data in primary and metastatic MB tissues was obtained and pooled from the Delattre, Gilbertson [39] and Thompson MB cohorts or obtained from the Cavalli et al. [8] and Pomeroy [40] cohorts. As cut-off for distinction between high versus low expression groups, the first versus last quartile was used as cut-off across each data set.

Proteomic data were kindly provided by Dr. Ernest Fraenkel (Broad Institute of MIT and Harvard, Boston, MA) [43] and were downloaded in the original instrument vendor format from the MassIVE online repository under MSV000082644.

ChIP-seq data for MYC (UCSC Accession: wgEncodeEH001867, wgEncodeEH002800, wgEncodeEH000670, wgEncodeEH003436, wgEncodeEH001807, wgEncodeEH000547, wgEncodeEH000545, wgEncodeEH002795, wgEncodeEH000596) were downloaded from ENCODE (Encyclopedia of DNA

Elements at UCSC [57, 58]) using the human genome GRCh 38/hg 38. ChIP-seq data were obtained from ENCODE [57, 58], and included data from six cell lines (Table S3). The files were combined into a single BAM file and data where then visualized using IGV version 2.9.1 (https://igv.org [59]).

DNA methylation data were downloaded from the GEO website (https://www.https://www.ncbi.nlm.nih.gov/geo/) for normal pediatric brain (GSE90871 [60]) and MB tissues (GSE85212 [61]). CpG sites included within nucleotides -1065 to +29,848 of *ElF4EBP1*, spanning the *ElF4EBP1* promoter region, two introns and three exons (human genome GRCh 37/hg19; Chr8: 37,886,955-37,917,868; exact chromosomal positions of the CpG sites are provided in Table S4) were selected for analysis and the mean was determined for each group and CpG site. A two-tailed Fisher's exact test was used to determine statistical differences between normal pediatric brain tissue samples and MB groups.

Analysis of MYC target genes co-expressed with *EIF4EBP1* was performed with R^2 AMC using the Cavalli et al. data set [8]. Genes co-expressed with *EIF4EBP1* (cut-off: r=0.45 and p<0.05) were initially identified for each MB group. GSEA was performed using the Broad 2020 09 c6 oncogenic gene set collection (p value cut-off: p<0.05). From these genes, the ones listed in the "Broad institute: MYC_UP_V1_UP" human gene dataset [44], considered as MYC target genes, were counted and the corresponding p value was calculated using Fisher's exact test.

Immunohistochemical staining for 4EBP1 protein expression

Immunohistochemistry for 4EBP1 was performed on formalin-fixed and paraffin-embedded (FFPE) MB tissue microarray (TMA) sections using standard protocols. The TMA consisted of tumor samples from 63 patients; samples were obtained after written informed consent and Institutional Review Board (IRB) approval between 1986 and 2012 from the BC Children's Hospital (BCCH, Vancouver, British Columbia, Canada) as previously described [45, 46]. Detailed information about this cohort, including methods for subgroup assignment, was previously published [46]. Two samples were excluded due to limited amounts of remaining tissue on the TMA. Sections were deparaffinized in xylene and rehydrated over a decreasing ethanol series before being incubated in Tris EDTA buffer (CC1 standard) at 95 °C for 1 h to retrieve antigenicity. Tissue sections were then incubated with the primary antibody against 4EBP1 (Abcam ab32024, 1:200) for 1 h (Ventana Discovery platform). Tissue sections with bound primary antibody were then incubated with the appropriate secondary antibody (Jackson antibodies at 1:500 dilution), followed by Ultramap HRP and Chromomap DAB detection. Intensity scoring was determined by an experienced pathologist and scored as positive and negative for the survival analyses. As for expression analysis in primary versus recurrent tissues, intensity scoring was performed according to a four-tiered scale: 0, no staining; 1, weakly positive staining; 2, moderately positive staining; 3, strongly positive staining. Immunohistochemical expression was quantified as H-score between 0-300 obtained by the product of the staining intensity (0-3) and the percentage of positive cells [62].

Statistical analyses

Unpaired t-tests were performed when comparing gene expression (unless otherwise stated). Correlation analyses were performed by calculating Pearson's correlation. GraphPad Prism version 7.04 (GraphPad Software, San Diego, CA, USA) was used for these statistical analyses. For correlative analysis of 4EBP1 staining with patient outcome, differences in survival between MB groups were calculated with log-rank tests for univariate survival analysis. Statistical analyses were performed with R 3.5.1 using the packages "survival" and "survminer" for survival analyses.

Cell culture

HEK293-T embryonic kidney cells were obtained from American Type Culture Collections (ATCC, Manassas, VA). Med8A cells were a kind gift from Prof. Pablo Landgraf (University Hospital Cologne, Cologne, Germany), and the HD-MB03 cell line was generously provided by Prof. Till Milde (DKFZ, Heidelberg, Germany). The generation of inducible control (ishScr) and stable 4EBP1 knock-down (ish4EBP1) Med8A and HD-MB03 cells has been reported elsewhere [25]. Control and MYC-overexpressing ONS76 and UW228.3 MB cells (as described in [49]) were kindly provided by Dr. Nan Qin (University Hospital Düsseldorf, Düsseldorf, Germany). HD-MB03 cells were maintained in Roswell Park

Memorial Institute (RPMI 1640) medium (61870010, Thermo Fisher Scientific, Waltham, MA, USA) supplemented with 10% fetal bovine serum (FBS) (10270-106, Thermo Fisher Scientific), 1% penicillin/streptomycin (10270-106, Sigma Aldrich, St Louis, USA) and 1% nonessential amino acids (MEM NEAA 100x) (11350912, Thermo Fisher Scientific). The remaining cell lines were maintained in Dulbecco's modified Eagle Medium (DMEM) (10569010, Thermo Fisher Scientific) supplemented with 10% FBS and 1% penicillin/streptomycin. All cell lines were cultured in a humidified incubator at 37 °C with 5% CO₂. The cell lines were confirmed to be mycoplasma-free by Venor GeM Classic (11-1050, Minerva Biolabs, Berlin, Germany) kit and validated by STR-profiling at the Genomics & Transcriptomics Laboratory (GTL), Biological and Medical Research Center (BMFZ), Heinrich Heine University (Düsseldorf, Germany).

siRNA transfection

Cells were transfected in 6-well plates at 70% confluency with 25 nM or 100 nM control siRNA (D-001206-14-50, Dharmacon, Cambridge, UK), 25 nM of two individual siRNAs targeting MYC (D-003282-14 & D-003282-35, Dharmacon) or 100 nM of a siRNA pool targeting MYC (L-003282-02-0010, Dharmacon) using siLentFect transfection reagent (1703362, Biorad, Hercules, CA, USA) (see Table S5 for siRNA sequences). Briefly, a master mix containing 125 μ l Opti-MEM (31985-070, Thermo Fisher Scientific) and 3 μ l siLentFect was prepared and incubated for 5 min at room temperature (RT). Meanwhile, 125 μ l Opti-MEM were mixed with 25 nM of siRNA for each well. The siRNA mix was mixed 1:1 with the master mix, incubated for 20 min at RT and added dropwise onto the cells. Medium was changed the day after transfected after 96 h. At 168 h following the first transfection, RNA and protein were harvested for further analysis. Cells transfected with the siRNA pool were used for further experiments after 72 h.

Plasmid construction

The pGL4.22 plasmid containing the -192 to +1372 promoter region of the human *EIF4EBP1* gene fused to Firefly Luciferase has been reported before [29]. Each of the three identified E boxes (MYC binding sites) was mutated separately to CAAGGC. Cloning was performed by GENEWIZ Germany GmbH (Leipzig, Germany).

Luciferase reporter assays

HEK 293-T cells were seeded in 12-well plates to reach 50% confluency on the day of transfection. Cells were transfected with 125 ng of the EIF4EBP1 promoter Firefly luciferase plasmid (wild type or mutants), 2 ng of Renilla luciferase expressing pRL SV40 plasmid (E2231, Promega; Madison, Wisconsin; USA), as internal control, and 25 ng, 50 ng or 100 ng of MYC expressing pcDNA3.3 MYC plasmid (kindly provided by Dr. Nan Qin, Düsseldorf, Germany), completed to 500 ng total DNA with pcDNA3.1 plasmid (V79020, Thermo Fisher Scientific) using CalFectinTM Cell Transfection Reagent (SL100478, SignaGen Laboratories, Frederick, MD; USA) according to the manufacturer's guidelines. Cells were harvested at 48 h post-transfection and activity of Firefly and *Renilla* luciferases were sequentially determined using the Dual-luciferase Reporter Assay System (E1980, Promega) and a Beckman Coulter microtiter plate reader (Beckman Coulter, Krefeld, Germany). All samples were performed in triplicate and the final luciferase quantification was formulated as the ratio of Firefly luciferase to Renilla luciferase luminescence. The relative luminescence was calculated by normalizing each biological replicate to either the 0 ng condition or to the EIF4EBP1 promoter control without mutations.

Cell proliferation

To assess cell proliferation, cells plated in 6-well plates were incubated in fresh medium containing 10 µM 5-ethynyl-2'-deoxyuridine (EdU) (Invitrogen) for 120 min at 37 °C. EdU staining was conducted using Click-iT™ EdU Pacific Blue™ Flow Cytometry Assay Kit (C10418, Invitrogen) according to the manufacturer's protocol. Briefly, cells were harvested, fixed with 4% paraformaldehyde in phosphate buffer saline (PBS) for 15 min, and permeabilized with 1X Click-iT™ saponin-based permeabilization reagent. Cells were incubated with a Click-iT™ reaction cocktail containing Click-iT™ reaction buffer, CuSO₄, Pacific Blue™ azide, and reaction buffer additive for 30 min while protected from light. Violet fluorescence intensity was measured with the BD FACSCantoTMII (BD Biosciences, Franklin Lakes, New Jersey, USA) using 405 nm excitation with a violet emission filter. Data analysis was performed with FlowJo 10 software (FlowJo).

Cell death assay

Cell death was measured by flow cytometry using propidium iodide (PI) staining. Briefly, attached and detached cells were harvested, centrifuged and resuspended in PBS containing 1 µg/ml PI (Sigma). Cell death quantification was performed using the BD FACSCantoTMII (BD Biosciences). A minimum of 10,000 events were recorded for each replicate. Data analysis was performed with FlowJo 10 software (FlowJo).

Migration assay

Using the OrisTM Cell Migration Assay (Platypus Technologies, Madison, WI, USA), Med8A and HD-MB03 were plated evenly around the provided cell stoppers with a final seeding concentration of 50,000 cells/100 µl/well in a 96-well plate. Cells were allowed to attach for 24 h, before cell stoppers were removed and plates were incubated for 72 h in an incubator at 37 °C with 5% CO₂. Med8A and HD-MB03 were stained with 30 µl of 5 mg/ml Hoechst 33342 (B2261, Sigma Aldrich, St. Louis, MO, USA) in PBS for 10 min and fluorescence was imaged using the CKX53 microscope (Olympus, Shinjuku, Japan) with DAPI filter. Pictures were taken using an ORCA-spark camera (Hamamatsu, Japan), the OLYMPUS cellSens program (Olympus) and cells were counted with ImageJ.

CellTiter-Glo assay

Cell viability of Med8A and HD-MB03 with ishRNA was measured using the CellTiter-Glo® luminescent cell viability assay according to the manufacturer's protocol (G7573, Promega). Briefly, cell viability was measured in technical replicates using 100 µl cell suspension per well in a white Nunc 96-well plate. Plain medium was used as blank. An equal volume of CellTiter-Glo® reagent was added to each well. The mix was incubated on an orbital shaker for 20 min protected from light. Luminescence was measured using the CLARIOstar (BMG Labtech, Ortenberg, Germany) plate reader.

Soft agar assay

Inducible control and stable 4EBP1 knock-down HD-MB03 and Med8A cells were treated with 1 μ g/ml doxycyclin 72 h prior to seeding. Cells were plated in 6-well plates with 8000 cells per well in DMEM supplemented with 10% FBS in a top layer of 0.25% agar added over a base layer of 0.4% agar in DMEM supplemented with 10% FBS. Cells were fed twice a week with 1 ml of either DMEM supplemented with 10% FBS, 1% penicillin/streptomycin and 1 μ g/ml doxycyclin (for Med8A) or RPMI supplemented with 10% FBS, 1% penicillin/streptomycin and 1 μ g/ml doxycyclin (for Hd8A) onto the top layer. After 3 weeks at 37 °C, colonies were stained with 0.01% crystal violet and 10 random fields were counted manually for each well. The percentage of colony-forming cells was calculated.

RNA extraction, cDNA synthesis and qRT-PCR

RNA was extracted using the RNeasy Plus Mini Kit (74136, QlAgen, Hilden, Germany). The extraction was performed according to the protocol provided by the manufacturer. Isolated RNA was retro-transcribed to cDNA using 1 μ g of RNA per reaction with either the QuantiTect Reverse Transcription Kit (205311, QlAgen) or the High-Capacity cDNA Reverse Transcription Kit (4368813, Applied Biosystems, Waltham, MA, USA) according to the manufacturer's protocol. Real-time PCR was performed in triplicates using 1 μ l cDNA and 9 μ l master mix consisting of 5 μ l SYBR Green PCR Mix (4309155, Applied Biosystems), 3 μ l H₂O and 1 μ l of forward and reverse primers (0.5 μ M final concentration). PPIA, GusB and β -actin were used as housekeepers. For primer sequences, see Table S6.

Protein extraction and immunoblot analysis

Cells were lysed in RIPA buffer (150 mM NaCl, 50 mM Tris-HCl, pH 8, 1% Triton X100, 0.5% Sodium deoxycholate, and 0.1% SDS) supplemented with proteinase inhibitor cocktail (11873580001, Roche, Basel, Switzerland) and phosphatase inhibitor (04906837001, Roche). Cell lysates were centrifuged at 14,000g for 15 min at 4 °C and supernatants were collected. Protein concentration was quantified using the PierceTM BCA Protein Assay Kit (23225, Thermo Fisher Scientific) according to the manufacturer's protocol. Twenty micrograms of total protein were loaded on a 12% polyacrylamide-SDS gel and transferred to a 0.2 µm nitrocellulose membrane (10600001, GE Healthcare, Chicago, IL, USA). Membranes were blocked with 5% bovine serum albumin (BSA) (8076.3, Carl Roth, Karlsruhe, Germany) TBS-Tween (20 mM Tris-HCl, pH 7.4, 150 mM NaCl, 0.1% Tween 20) and probed with primary antibodies (as

detailed in Table S7) diluted 1:1000 in 5% BSA TBS overnight at 4 °C. Membranes were then incubated with either a corresponding antimouse (926-32210, Li-Cor, Bad Homburg, Germany) or anti-rabbit (926-32211, Li-Cor) fluorescent secondary antibody diluted 1:10,000 or a corresponding anti-rabbit IgG, HRP-linked secondary antibody (7074, Cell Signaling, Cambridge, UK) diluted 1:3000. The fluorescent signal was visualized with the LI-COR Odyssey® CLx system (Li-Cor) and the chemiluminescent signal was detected using enhanced chemiluminescent reagent (ECL) and the detection device LAS-3000 mini (Fujifilm, Tokyo, Japan).

Statistical analysis of experimental data

All experiments were carried out in three biological replicates. Data are represented as mean +/- standard deviation (SD). A two-sided Student's t-test was used to compare differences between control and experimental groups. Results were considered as being statistically significant at p < 0.05. Statistical tests were calculated with GraphPad Prism version 7.04.

REFERENCES

- Ostrom QT, Price M, Ryan K, Edelson J, Neff C, Cioffi G, et al. CBTRUS Statistical Report: Pediatric Brain Tumor Foundation Childhood and Adolescent Primary Brain and Other Central Nervous System Tumors Diagnosed in the United States in 2014-2018. Neuro Oncol. 2022;24:iii1-iii38. https://doi.org/10.1093/neuonc/ noac161
- Taylor MD, Northcott PA, Korshunov A, Remke M, Cho YJ, Clifford SC, et al. Molecular subgroups of medulloblastoma: the current consensus. Acta Neuropathologica. 2012;123:465–72. https://doi.org/10.1007/s00401-011-0922-z
- 3. Louis DN, Perry A, Reifenberger G, von Deimling A, Figarella-Branger D, Cavenee WK, et al. The 2016 World Health Organization Classification of Tumors of the Central Nervous System: a summary. Acta Neuropathol. 2016;131:803–20. https://doi.org/10.1007/s00401-016-1545-1
- Louis DN, Perry A, Wesseling P, Brat DJ, Cree IA, Figarella-Branger D, et al. The 2021 WHO Classification of Tumors of the Central Nervous System: a summary. Neuro Oncol. 2021;23:1231–51. https://doi.org/10.1093/neuonc/noab106
- Northcott PA, Robinson GW, Kratz CP, Mabbott DJ, Pomeroy SL, Clifford SC, et al. Medulloblastoma. Nat Rev Dis Primers. 2019;5:11 https://doi.org/10.1038/s41572-019-0063-6
- Northcott PA, Korshunov A, Witt H, Hielscher T, Eberhart CG, Mack S, et al. Medulloblastoma comprises four distinct molecular variants. Journal of Clinical Oncology. 2011;29:1408–14. https://doi.org/10.1200/JCO.2009.27.4324
- Northcott PA, Buchhalter I, Morrissy AS, Hovestadt V, Weischenfeldt J, Ehrenberger T, et al. The whole-genome landscape of medulloblastoma subtypes. Nature. 2017;547:311–7. https://doi.org/10.1038/nature22973
- Cavalli FMG, Remke M, Rampasek L, Peacock J, Shih DJH, Luu B, et al. Intertumoral heterogeneity within medulloblastoma subgroups. Cancer Cell. 2017;31:737–54 e736. https://doi.org/10.1016/j.ccell.2017.05.005
- Sharma T, Schwalbe EC, Williamson D, Sill M, Hovestadt V, Mynarek M, et al. Second-generation molecular subgrouping of medulloblastoma: an international meta-analysis of Group 3 and Group 4 subtypes. Acta Neuropathol. 2019;138:309–26. https://doi.org/10.1007/s00401-019-02020-0
- Kawauchi D, Robinson G, Uziel T, Gibson P, Rehg J, Gao C, et al. A mouse model of the most aggressive subgroup of human medulloblastoma. Cancer Cell. 2012;21:168–80. https://doi.org/10.1016/j.ccr.2011.12.023
- Pei Y, Moore CE, Wang J, Tewari AK, Eroshkin A, Cho YJ, et al. An animal model of MYC-driven medulloblastoma. Cancer Cell. 2012;21:155–67. https://doi.org/ 10.1016/j.ccr.2011.12.021
- Roussel MF, Robinson GW. Role of MYC in Medulloblastoma. Cold Spring Harb Perspect Med. 2013;3:a014308.
- Das SK, Lewis BA, Levens D. MYC: a complex problem. Trends Cell Biol. 2023;33:235–46. https://doi.org/10.1016/j.tcb.2022.07.006
- Tameire F, Verginadis II, Leli NM, Polte C, Conn CS, Ojha R, et al. ATF4 couples MYC-dependent translational activity to bioenergetic demands during tumour progression. Nat Cell Biol. 2019;21:889–99. https://doi.org/10.1038/s41556-019-0347-9
- Balakumaran BS, Porrello A, Hsu DS, Glover W, Foye A, Leung JY, et al. MYC activity mitigates response to rapamycin in prostate cancer through eukaryotic initiation factor 4E-binding protein 1-mediated inhibition of autophagy. Cancer Res. 2009;69:7803–10. https://doi.org/10.1158/0008-5472.CAN-09-0910
- Musa J, Orth MF, Dallmayer M, Baldauf M, Pardo C, Rotblat B, et al. Eukaryotic initiation factor 4E-binding protein 1 (4E-BP1): a master regulator of mRNA translation involved in tumorigenesis. Oncogene. 2016;35:4675–88. https:// doi.org/10.1038/onc.2015.515

- Liu GY, Sabatini DM. mTOR at the nexus of nutrition, growth, ageing and disease.
 Nat Rev Mol Cell Biol. 2020;21:183–203. https://doi.org/10.1038/s41580-019-0199-v
- Valvezan AJ, Manning BD. Molecular logic of mTORC1 signalling as a metabolic rheostat. Nat Metab. 2019:1:321–33. https://doi.org/10.1038/s42255-019-0038-7
- Lazaris-Karatzas A, Montine KS, Sonenberg N. Malignant transformation by a eukaryotic initiation factor subunit that binds to mRNA 5' cap. Nature. 1990;345:544–7. https://doi.org/10.1038/345544a0
- Dowling RJO, Topisirovic I, Alain T, Bidinosti M, Fonseca BD, Petroulakis E, et al. mTORC1-mediated cell proliferation, but not cell growth, controlled by the 4E-BPs. Science (New York, N.Y.). 2010;328:1172–6. https://doi.org/10.1126/science 1187532
- Ding M, Van der Kwast TH, Vellanki RN, Foltz WD, McKee TD, Sonenberg N, et al. The mTOR Targets 4E-BP1/2 restrain tumor growth and promote hypoxia tolerance in PTEN-driven prostate cancer. Mol Cancer Res. 2018;16:682–95. https://doi.org/10.1158/1541-7786.MCR-17-0696
- Wang Z, Feng X, Molinolo AA, Martin D, Vitale-Cross L, Nohata N, et al. 4E-BP1 is a tumor suppressor protein reactivated by mtor inhibition in head and neck cancer. Cancer Res. 2019;79:1438–50. https://doi.org/10.1158/0008-5472.CAN-18-1220
- Braunstein S, Karpisheva K, Pola C, Goldberg J, Hochman T, Yee H, et al. A hypoxia-controlled cap-dependent to cap-independent translation switch in breast cancer. Molecular Cell. 2007;28:501–12. https://doi.org/10.1016/ i.molcel.2007.10.019
- Lee M, Kim EJ, Jeon MJ. MicroRNAs 125a and 125b inhibit ovarian cancer cells through post-transcriptional inactivation of EIF4EBP1. Oncotarget. 2016;7:8726–42. https://doi.org/10.18632/oncotarget.6474
- Levy T, Voeltzke K, Hauffe L, Alasad K, Snaebjörnsson M, Marciano R, et al. 4EBP1/ 2 support tumorigenicity and cell survival during energetic stress by translationally regulating fatty acid synthesis. bioRxiv https://doi.org/10.1101/ 2022.09.09.507243.
- Petroulakis E, Parsyan A, Dowling RJO, LeBacquer O, Martineau Y, Bidinosti M, et al. p53-dependent translational control of senescence and transformation via 4E-BPs. Cancer Cell. 2009;16:439–46. https://doi.org/10.1016/ j.ccr.2009.09.025
- Funk CM, Orth MF, Aljakouch K, Ehlers A, Li J, Hölting TLB, et al. Chromosome 8 gain drives poor patient outcome via expression of 4E-BP1 in Ewing sarcoma. bioRxiv https://doi.org/10.1101/2022.12.11.519935.
- Wu S, Wagner G. Deep computational analysis details dysregulation of eukaryotic translation initiation complex eIF4F in human cancers. Cell Syst. 2021;12:907–23 e906. https://doi.org/10.1016/j.cels.2021.07.002
- Voeltzke K, Scharov K, Funk CM, Kahler A, Picard D, Hauffe L, et al. EIF4EBP1 is transcriptionally upregulated by MYCN and associates with poor prognosis in neuroblastoma. Cell Death Discov. 2022;8:157 https://doi.org/10.1038/s41420-022-00963-0
- Karlsson E, Perez-Tenorio G, Amin R, Bostner J, Skoog L, Fornander T, et al. The mTOR effectors 4EBP1 and S6K2 are frequently coexpressed, and associated with a poor prognosis and endocrine resistance in breast cancer: a retrospective study including patients from the randomised Stockholm tamoxifen trials. Breast Cancer Res. 2013;15:R96 https://doi.org/10.1186/bcr3557
- Rutkovsky AC, Yeh ES, Guest ST, Findlay VJ, Muise-Helmericks RC, Armeson K, et al. Eukaryotic initiation factor 4E-binding protein as an oncogene in breast cancer. BMC Cancer. 2019;19:491 https://doi.org/10.1186/s12885-019-5667-4
- 32. Cha YL, Li PD, Yuan LJ, Zhang MY, Zhang YJ, Rao HL, et al. EIF4EBP1 over-expression is associated with poor survival and disease progression in patients with hepatocellular carcinoma. PLoS ONE. 2015;10:e0117493 https://doi.org/10.1371/journal.pone.0117493
- Chao MW, Wang LT, Lai CY, Yang XM, Cheng YW, Lee KH, et al. elF4E binding protein 1 expression is associated with clinical survival outcomes in colorectal cancer. Oncotarget. 2015;6:24092–104. https://doi.org/10.18632/ oncotarget.4483
- Wu CC, Hou S, Orr BA, Kuo BR, Youn YH, Ong T, et al. mTORC1-Mediated Inhibition of 4EBP1 Is Essential for Hedgehog Signaling-Driven Translation and Medulloblastoma. Dev Cell. 2017;43:673–88e675. https://doi.org/10.1016/j.devcel.2017.10.011
- 35. Forget A, Martignetti L, Puget S, Calzone L, Brabetz S, Picard D, et al. Aberrant ERBB4-SRC signaling as a Hallmark of group 4 medulloblastoma revealed by integrative phosphoproteomic profiling. Cancer Cell. 2018;34:379–95e377. https://doi.org/10.1016/j.ccell.2018.08.002
- Liu Y, Horn JL, Banda K, Goodman AZ, Lim Y, Jana S, et al. The androgen receptor regulates a druggable translational regulon in advanced prostate cancer. Sci Transl Med. 2019;11:eaaw4993.
- Hauffe L, Picard D, Musa J, Remke M, Grunewald TGP, Rotblat B, et al. Eukaryotic translation initiation factor 4E binding protein 1 (EIF4EBP1) expression in glioblastoma is driven by ETS1- and MYBL2-dependent transcriptional activation. Cell Death Discov. 2022;8:91 https://doi.org/10.1038/s41420-022-00883-z

- Northcott PA, Shih DJ, Peacock J, Garzia L, Morrissy AS, Zichner T, et al. Subgroupspecific structural variation across 1,000 medulloblastoma genomes. Nature. 2012;488:49–56. https://doi.org/10.1038/nature11327
- Robinson G, Parker M, Kranenburg TA, Lu C, Chen X, Ding L, et al. Novel mutations target distinct subgroups of medulloblastoma. Nature. 2012;488:43–8. https://doi.org/10.1038/nature11213
- Cho YJ, Tsherniak A, Tamayo P, Santagata S, Ligon A, Greulich H, et al. Integrative genomic analysis of medulloblastoma identifies a molecular subgroup that drives poor clinical outcome. J Clin Oncol. 2011;29:1424–30. https://doi.org/10.1200/ ICO 2010 28 5148
- Kool M, Koster J, Bunt J, Hasselt NE, Lakeman A, van Sluis P, et al. Integrated genomics identifies five medulloblastoma subtypes with distinct genetic profiles, pathway signatures and clinicopathological features. PLoS ONE. 2008;3:e3088 https://doi.org/10.1371/journal.pone.0003088
- Hovestadt V, Ayrault O, Swartling FJ, Robinson GW, Pfister SM, Northcott PA. Medulloblastomics revisited: biological and clinical insights from thousands of patients. Nat Rev Cancer. 2020;20:42–56. https://doi.org/10.1038/s41568-019-0223-8
- Archer TC, Ehrenberger T, Mundt F, Gold MP, Krug K, Mah CK, et al. Proteomics, post-translational modifications, and integrative analyses reveal molecular heterogeneity within medulloblastoma subgroups. Cancer Cell. 2018;34:396–410 e398. https://doi.org/10.1016/j.ccell.2018.08.004
- Bild AH, Yao G, Chang JT, Wang Q, Potti A, Chasse D, et al. Oncogenic pathway signatures in human cancers as a guide to targeted therapies. Nature. 2006;439:353–7. https://doi.org/10.1038/nature04296
- Delaidelli A, Dunham C, Santi M, Negri GL, Triscott J, Zheludkova O, et al. Clinically tractable outcome prediction of non-WNT/Non-SHH medulloblastoma based on TPD52 IHC in a multicohort study. Clin Cancer Res. 2022;28:116–28. https:// doi.org/10.1158/1078-0432.CCR-21-2057
- Triscott J, Lee C, Foster C, Manoranjan B, Pambid MR, Berns R, et al. Personalizing the treatment of pediatric medulloblastoma: Polo-like kinase 1 as a molecular target in high-risk children. Cancer Res. 2013;73:6734–44. https://doi.org/10.1158/ 0008-5472.CAN-12-4331
- 47. Graff JR, Konicek BW, Lynch RL, Dumstorf CA, Dowless MS, McNulty AM, et al. eIF4E activation is commonly elevated in advanced human prostate cancers and significantly related to reduced patient survival. Cancer Res. 2009;69:3866–73. https://doi.org/10.1158/0008-5472.CAN-08-3472
- 48. O'Reilly KE, Warycha M, Davies MA, Rodrik V, Zhou XK, Yee H, et al. Phosphorylated 4E-BP1 is associated with poor survival in melanoma. Clin Cancer Res. 2009;15:2872–8. https://doi.org/10.1158/1078-0432.CCR-08-2336
- Qin N, Paisana E, Langini M, Picard D, Malzkorn B, Custodia C, et al. Intratumoral heterogeneity of MYC drives medulloblastoma metastasis and angiogenesis. Neuro Oncol. 2022;24:1509–23. https://doi.org/10.1093/neuonc/noac068
- Jeon SM, Chandel NS, Hay N. AMPK regulates NADPH homeostasis to promote tumour cell survival during energy stress. Nature. 2012;485:661–5. https://doi.org/ 10.1038/nature11066
- Leprivier G, Remke M, Rotblat B, Dubuc A, Mateo AR, Kool M, et al. The eEF2 kinase confers resistance to nutrient deprivation by blocking translation elongation. Cell. 2013;153:1064–79. https://doi.org/10.1016/j.cell.2013.04.055
- Bennett CD, Kohe SE, Gill SK, Davies NP, Wilson M, Storer LCD, et al. Tissue metabolite profiles for the characterisation of paediatric cerebellar tumours. Sci Rep. 2018;8:11992 https://doi.org/10.1038/s41598-018-30342-8
- Meley D, Spiller DG, White MR, McDowell H, Pizer B, See V. p53-mediated delayed NF-kappaB activity enhances etoposide-induced cell death in medulloblastoma. Cell Death Dis. 2010;1:e41 https://doi.org/10.1038/cddis.2010.16
- Kuzuoglu-Ozturk D, Aksoy O, Schmidt C, Lea R, Larson JD, Phelps RRL, et al. N-myc-Mediated Translation Control Is a Therapeutic Vulnerability in Medulloblastoma. Cancer Res. 2023;83:130–40. https://doi.org/10.1158/0008-5472.CAN-22-0945
- Palm W, Park Y, Wright K, Pavlova NatalyaN, Tuveson David A, Thompson Craig B.
 The utilization of extracellular proteins as nutrients is suppressed by mTORC1.
 Cell. 2015;162:259–70. https://doi.org/10.1016/j.cell.2015.06.017
- Kumar S, Sharife H, Kreisel T, Mogilevsky M, Bar-Lev L, Grunewald M, et al. Intratumoral metabolic zonation and resultant phenotypic diversification are dictated by blood vessel proximity. Cell Metab. 2019;30:201–11e206. https://doi.org/ 10.1016/j.cmet.2019.04.003
- Davis CA, Hitz BC, Sloan CA, Chan ET, Davidson JM, Gabdank I, et al. The Encyclopedia of DNA elements (ENCODE): data portal update. Nucleic Acids Res. 2018;46:D794–D801. https://doi.org/10.1093/nar/gkx1081
- 58. Consortium EP. An integrated encyclopedia of DNA elements in the human genome. Nature. 2012;489:57–74. https://doi.org/10.1038/nature11247
- Robinson JT, Thorvaldsdottir H, Winckler W, Guttman M, Lander ES, Getz G, et al. Integrative genomics viewer. Nature biotechnology. 2011;29:24–26. https://doi.org/10.1038/nbt.1754

- Chatterton Z, Hartley BJ, Seok MH, Mendelev N, Chen S, Milekic M, et al. In utero exposure to maternal smoking is associated with DNA methylation alterations and reduced neuronal content in the developing fetal brain. Epigenetics Chromatin. 2017;10:4 https://doi.org/10.1186/s13072-017-0111-y
- Pai S, Li P, Killinger B, Marshall L, Jia P, Liao J, et al. Differential methylation of enhancer at IGF2 is associated with abnormal dopamine synthesis in major psychosis. Nat Commun. 2019;10:2046 https://doi.org/10.1038/s41467-019-09786-7
- McCarty KS Jr, Miller LS, Cox EB, Konrath J, McCarty KS Sr. Estrogen receptor analyses. Correlation of biochemical and immunohistochemical methods using monoclonal antireceptor antibodies. Arch Pathol Lab Med. 1985:109:716–21.
- Roth RB, Hevezi P, Lee J, Willhite D, Lechner SM, Foster AC, et al. Gene expression analyses reveal molecular relationships among 20 regions of the human CNS. Neurogenetics. 2006;7:67–80. https://doi.org/10.1007/s10048-006-0032-6
- 64. de Bont JM, Kros JM, Passier MM, Reddingius RE, Sillevis Smitt PA, et al. Differential expression and prognostic significance of SOX genes in pediatric meduloblastoma and ependymoma identified by microarray analysis. Neuro Oncol. 2008;10:648–60. https://doi.org/10.1215/15228517-2008-032
- Ho DM, Shih CC, Liang ML, Tsai CY, Hsieh TH, Tsai CH, et al. Integrated genomics has identified a new AT/RT-like yet INI1-positive brain tumor subtype among primary pediatric embryonal tumors. BMC Med Genomics. 2015;8:32 https:// doi.org/10.1186/s12920-015-0103-3

ACKNOWLEDGEMENTS

The authors would like to acknowledge the ENCODE Consortium and the Vishwanath lyer, Sherman Weissman, and Michael Snyder laboratories for generating the respective datasets. G.L. was supported by grants from the Deutsche Forschungsgemeinschaft (grant no. LE 3751/2-1), the German Cancer Aid (grant no. 70115129), the Elterninitiative Düsseldorf e.V. (grant no. 701910003), the Dr. Rolf M. Schwiete Stiffung (grant no. 2020-018), the Brigitte und Dr. Konstanze Wegener Foundation (A 2023 #11) and the Research Commission of the Medical Faculty, Heinrich Heine University Düsseldorf (grant no. 2020-044). LH was funded by the Dr. Rolf M. Schwiete Stiftung (grant no. 2020-018) and the Brigitte und Dr. Konstanze Wegener Foundation (A 2023 #11).

AUTHOR CONTRIBUTIONS

Conceptualization: LH, KS, BR, and GL; Methodology: LH, KS, AD, and GL; Investigation: LH, KS, AD, DP, OL, and ML; Resources: AD, CD, and PHBS; Writing: LH and GL; Visualization: LH, KS, AD, and GL; Supervision: TR, CP, PHBS, GR, MR, and GL; Funding Acquisition: LH and GL.

FUNDING

Open Access funding enabled and organized by Projekt DEAL.

COMPETING INTERESTS

The authors declare no competing interests.

ETHICS APPROVAL

The BC Children's Hospital (BCCH) cohort consists of medulloblastoma samples prospectively obtained, after written informed consent and Institutional Review Board (IRB) approval, between 1986 and 2012 from the BC BCCH (Vancouver, British Columbia, Canada) as previously described [45, 46].

ADDITIONAL INFORMATION

Supplementary information The online version contains supplementary material available at https://doi.org/10.1038/s41420-025-02601-x.

Correspondence and requests for materials should be addressed to Gabriel Leprivier.

Reprints and permission information is available at http://www.nature.com/reprints

Publisher's note Springer Nature remains neutral with regard to jurisdictional claims in published maps and institutional affiliations.

Open Access This article is licensed under a Creative Commons Attribution 4.0 International License, which permits use, sharing, adaptation, distribution and reproduction in any medium or format, as long as you give appropriate credit to the original author(s) and the source, provide a link to the Creative Commons licence, and indicate if changes were made. The images or other third party material in this article are included in the article's Creative Commons licence, unless indicated otherwise in a credit line to the material. If material is not included in the article's Creative Commons licence and your intended use is not permitted by statutory regulation or exceeds the permitted use, you will need to obtain permission directly from the copyright holder. To view a copy of this licence, visit http://creativecommons.org/licenses/by/4.0/.

© The Author(s) 2025